Journal of Engineering Science and Technology
Vol. 15, No. 6 (2020) 4367 – 4382

EXPERIMENTAL EVALUATION OF BOND STRENGTH PERFORMANCE BETWEEN NORMAL CONCRETE SUBSTRATE AND DIFFERENT OVERLAY MATERIALS

MUNA M. AL-RUBAYE*, RANA F. YOUSEF, HAITHAM H. MUTEB

Department of Civil Engineering, College of Engineering,
University of Babylon, Babylon 6 Hillah, 51002, Iraq
*Corresponding Author: eng.muna.mohammed@uobabylon.edq.iq

Abstract

This research was implemented to evaluate the effect of different concrete mixes and commercial repair binders as overlay materials on the interfacial bond strength. Experimental work was conducted on a series of composite samples that were made of two different concretes; the substrate is made of normal strength concrete and various types of the overlay materials. Six different mixes for the concrete and the mortar were used as the overlay materials such as normal concrete as a reference interface, ultra- high performance fiber concrete, reactive powder concrete and self-compacting mortar. Two commercial repair binders that are non-shrink cementitious and shrinkage compensated micro concrete were also used. Three roughness surfaces of the substrate have been taken into consideration: grooves, drill holes and as-cast. The bond performance was assessed via two tests: the slant shear test and direct shear test at ages of composite specimens of 1, 7, and 28 days. The results showed that, the ultra- high performance fiber concrete has a very good bond quality with the substrate, whereas the contribution of the rest materials to the bond strength is in the next order: reactive powder concrete, self-compacting mortar, shrinkage compensated micro concrete, non-shrink cementitious and normal strength concrete.

Keywords: Bi-surface shear test, Overlay materials, Roughness surfaces, Slant shear test, Substrate concrete.

1. Introduction

A good bonding strength between two concretes interfaces plays an important role in the enhancement of long-term durability and ensures that the two concretes act monolithically. Besides, providing an adequate bond is considered as a key factor for a reliable load transfer between different concrete layers as it provides enough strength to resist the mechanical loading stress as well as maintains an extended service-life performance [1-3]. The interfaces between two concretes are existing in the reinforced concrete structures when the strengthening and repair processes are conducted or when the precast concrete elements with cast-in-place portions are utilized [4-6]. The concrete-to-concrete bond strength is influenced by many factors such as the mechanical properties of the two concretes, the roughness of the substrate surface, the moisture presence at the substrate surface before the casting of the overlay material and the test method that utilized to evaluate the bond strength [7-9]. The bond strength as well depends on the type of the overlay that contributes to both the load-carrying capacity and the stiffness of the structural element in addition to improving the durability [10-13]. The cementitious materials (strengthening and repair materials) has made progress in different implementations such as toppings; in particular, when they used as rehabilitation materials, connecting precast parts, and overlay for bridges, accordingly, the demand for those materials has increased [14-16]. Furthermore, the bond strength depends on important parameters describing the material interface strength when there is no reinforcement at the interface between two concretes: cohesion and the friction, which are the shear strength and a degree of the shearing resistance [17].

To evaluate the bond performance between different concretes interfaces, various test methods are available such as pull off test, splitting tensile test, the direct shear test and the slant shear test [18-21], however, in the present study only two methods were adapted, which are slant shear test [18] and direct shear test [22]. Figure 1 shows the geometry of two different shapes of specimens (cylinder and cube) that were used in the slant shear test and direct shear test. The former test is widely accepted due to its realistic representation of the actual state of shear stress that the real structures are subjected to because the bonding surface is subjected to compression and shear stresses during loading. The bonded interface of the composite sample for this method arranged at some inclination is subjected to a compressive force (Fig. 1(a)). Regarding the latter test, the bond strength is normally measured under shear stresses, thus, it is simulating the states of shear stress that exist in the real structures. However, in most cases, the bonded surface is subjected to shear stress with a small bending stress. To overcome this shortcoming, a test method was developed that is so-called as bi-surface shear test in which the loads are applied symmetrically. Furthermore, the combination of loading and the size of specimen causes a state of shear stress that represents the state of stress occurred in many structures as shown in Fig. 1(b) [22; 23].

The bond strength between two types of concrete has been actively studied [9; 24-26], however, these studies were conducted on the composite specimens comprised of substrate and only one overlay material. In this paper, the slant shear test and bi-surface shear test were carried out to evaluate the effect of different concrete mixes that produced from local materials and commercial repair binders as the overlay materials on the interfacial bond strength. In addition, the effect of roughness surfaces of the substrate and age of composite specimens on the bond

strength was evaluated. The outcomes of this study would be helpful on choosing the appropriate material that indeed leads to a better interface bond strength.

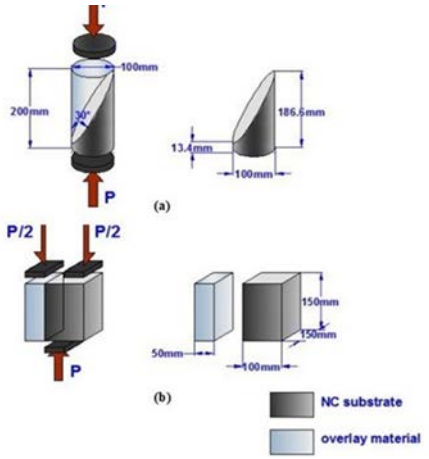

Fig. 1. Dimensions of specimens for (a) Slant shear test (b) Bi-surface shear test.

2. Experimental Work

Each of tested specimens consisted of two differently concrete, which are the NC substrate and overlay material. Many studied parameters have been considered that are the type of the overlay material, test method, the substrate roughness, and the age of the composite specimens.

2.1. Materials

All materials used to prepare NC substrate and the overlay materials mixes were locally available. The Portland limestone cement (PLC) has been utilized in this study. Al-Ekhaider sand was used as a fine aggregate (FA) in the substrate concrete mixes with a maximum size of particles 5 mm. In ultra- high-performance fiber concrete (UHPFC) and reactive powder concrete (RPC) mixes, the nominal size of the fine aggregate ranges from (150 to 600) μm, which is prepared by sieving the sand to satisfy the grading according to the requirements. The fine aggregate is clean, free from loam and clay and it is conformed to the standard specification [27]. Coarse aggregate (CA) used in the substrate concrete mixes is of maximum size equal to 12.5 mm and it conformed to the standard specification [27].

The UHPFC and RPC mixes were also incorporating micro steel fibers (MSF), super–plasticizer (SP), and silica fume (SF). The MSF used with length of 13 mm and diameter of 0.2 mm; it is clean of rust or oil. This type of MSF is straight brass-coated micro steel fibers. The SP used was a third generation super plasticizer which is known commercially as Hyperplast (SP-PC200) for concrete and mortar to fluidize the dry mix, it is an aqueous solution of modified polycarboxylic polymers with long chains, free from chlorides and complies with [28]. The SF used in this study of (0.1 to 1 μm) particle size and it is less than the average cement particle by about 100 times, it conformed to the physical and chemical requirements of [29]. The limestone powder (LP) used as a filler with maximum particle size of

125 μm was used in self-compacting mortar (SCM) mixes to increase the paste volume to lubricate the aggregate particles.

2.2. Normal concrete substrate and overlays mixes properties

To achieve the aim of this study, it was decided to consider the same mix design for the NC substrate and six different mixes for overlay materials. The mix proportion for the NC substrate has been designed to achieve compressive strength of 32 MPa at 28 days. On the other hand, different mixes for either concrete or mortar have been used as the overlay materials, these materials including: UHPFC, RPC, SCM, two commercial repair binders, and NC as a reference interface. The typical mix composition of UHPFC and RPC includes five constituents that are the cement, sieved and dried FA ranges from (150 to 600) μm, the SF, MSF and SP-PC200. Generally, self-compacting concrete (SCC) or SCM requires higher cement content than NC. The SCM mix was developed based on the reference SCM mix designed by Tuaum et al. [30]. The SCM mix consists of LP as a filler to enhance the flowability and durability, reduce the amount of cement and heat of hydration, and SP-PC200 to increase segregation resistance and lower yield stress of SCM. Further, FA with particles of a maximum size of 2.36 mm has been used.

The repair binders are pre-mixed and pre-packed in bags containing the solid fraction. Shrinkage compensated micro concrete (Cempatch FL) and non-shrink cementitious (Flo-Grout 2) are composed of cementitious materials, additives, with fine aggregates and a blend of dry powders with selected aggregates respectively. To obtain a desirable flow they have been mixed with a specific amount of water according to the manufacturer's recommendations. To provide 28-day compressive strength of 62 MPa, the Flo-Grout 2 and Cempatch FL require water to solids ratio (w/s) of 0.18 and 0.13 respectively. The amounts of the ingredients used in the NC substrate, UHPFC, RPC and SCM mixes are given in Table 1.

Table 1. Mix proportions of NC substrate and different overlay materials, kg/m^3.

Constituents	NC	UHPFC	RPC	SCM
PLC	445	780	960	625
FA	680	920	1040	1185
CA	1024			
Water	200	150	190	208
MSF		157	157	
SF		200	240	
LP				138
SP- PC200		40	75	64
Mix strength grade, MPa at 28 days	32	150	128	60.23

2.3. Preparation of composite specimens

Series of composite specimens of NC substrate-to- different concrete or mortar overlay materials were made and tested. For comparison, control specimens of NC substrate-to-NC overlay were also made and tested. The slant shear test and the bi-

surface shear test have been adopted to evaluate the interface bond strength at ages 1, 7, and 28 days. Regarding the former test, the specimens were 100×200 mm cylinders with an inclination angle (α) of 30° that measured with respect to the vertical axis [31]. The later test specimens were cubes with 150mm, two third of cubes was the NC substrate and one third was the overlay material [22]. To made NC substrate concrete specimens in these fashions, wood cylinders were cut in the slanted dimension of the cylinder form and the specified orientation and wood cubes with a height of 150 mm and a base size of 50×150 mm as shown in Figs. 2 and 3 respectively.

Fig. 2. Wood slices for slant shear test.

Fig. 3. Wood slices for bi-surface shear test.

First, half of the cylinders moulds and two third of cubes moulds were occupied by the casted NC substrate, then the fresh NC substrate mixes were left in the moulds for 24 hours. Thereafter, the specimens were demoulded and were cured in water for 28 days. After curing, three surface preparation methods are applied on NC substrate specimens; as-cast, the drill holes and grooving.

Beushausen et al. [32] reported that it is necessary to obtain the saturated surface dried (SSD) conditions of the NC substrate interface before the application of the overlay by wetting the NC substrate interface. The reason behind this is when applying a fresh overlay upon the dry NC substrate causes migrate the mixing water from the fresh overlay to the substrate. The interfaces of NC substrate-overlays were moisten and then swabbed dry by a wet cloth. The SSD slant shear test specimens were put into the cylinders moulds with the slant side face upward, then the utilized overlay materials was applied over top of the NC substrate concrete to

complete these cylinders. On the other hand, the SSD bi-surface shear test specimens were placed into the cubes moulds, and the overlay material, which constitutes one third of the cubes, was applied to complete these cubes.

The full composite NC substrate-overlay cylinders and cubes were then tested in compression to determine the interfacial bond strength as shown in Figs. 4 and 5. Regarding the bi-surface shear test, the composite cubes were loaded symmetrically at three points using 25 mm-thick, 50 mm wide and 150 mm long steel plates [22]. Since an important characteristic of composite substrate-overlay specimens is early bond strength, the interface bond strengths were obtained at one day, seven days, and in addition to the standard 28 days.

Fig. 4. Test setup for slant shear test.

Fig. 5. Test setup for bi-surface shear test.

3. Results and Discussion

3.1. Bond strength

The bond strength values of the composite NC substrate-overlay specimens have been obtained through the slant shear and bi-surface shear tests; those values represent the average bond strengths. The slant shear strengths have been obtained through dividing the maximum applied force by the elliptical bonded area. According to the bi-surface shear test, the bonding shear strength has been calculated through dividing the maximum applied force by the bonded surface area as Equation (1) shows.

$$f_s = \frac{F}{A} \quad (1)$$

where *fs* is the bond shear strength (MPa), *F* is the maximum applied force, *N* and *A* is the bonded surface area, mm^2.

Figure 6 displays the interface view of the six composite specimens with different surface treatments after testing them by slant shear test and bi-surface shear test. It can be seen that the grooves and drill holes of NC-overlay treated surface were clear and feature, with some overlay remained in the grooves and drill holes.

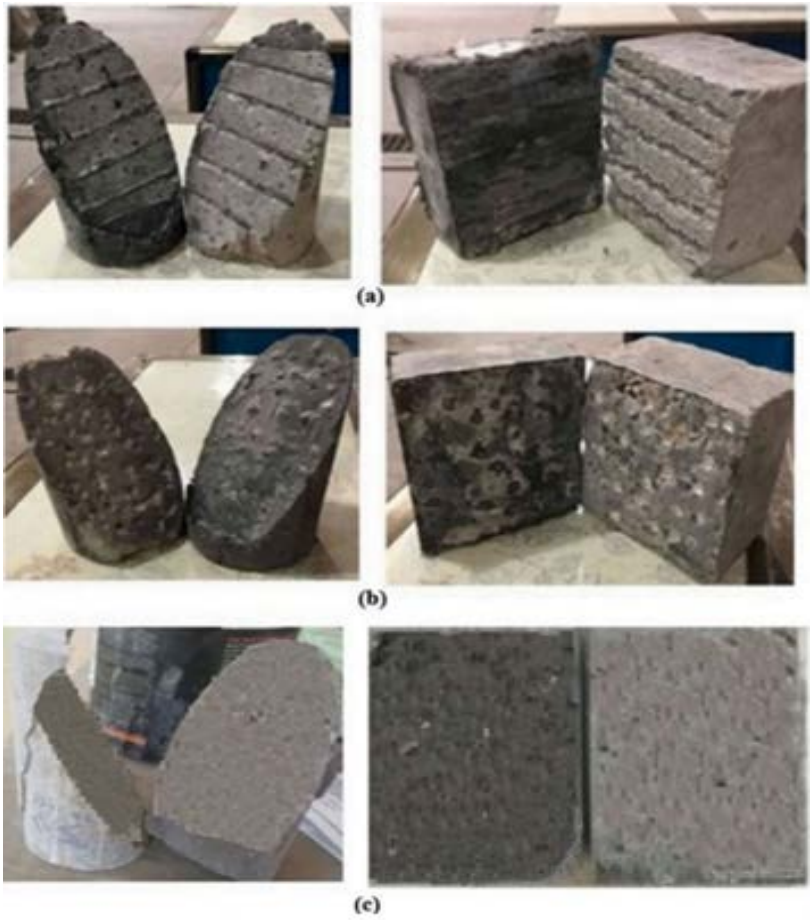

Fig. 6. Interface view of composite specimens after testing (a) Grooved, (b) Drill holes, and (c) As-cast surface.

Figures 7, 8, and 9 present the average slant shear strengths, whilst Figs. 10, 11, and 12 show the average bi-surface shear strengths with surface preparations of grooved, drill holes and as-cast at 1 day, 7days and 28 days. It can be seen from these Figs. that the bond strengths by slant shear method were higher than those measured by bi-surface shear method for all overlay materials and surface preparations. These is due to the higher friction forces and interlock that result from high compressive stresses that occur in slant shear test, which increase the shear failure load [23].

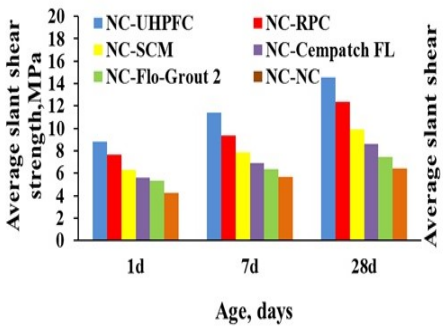

Fig. 7. Average slant shear strengths for the grooved substrate surface.

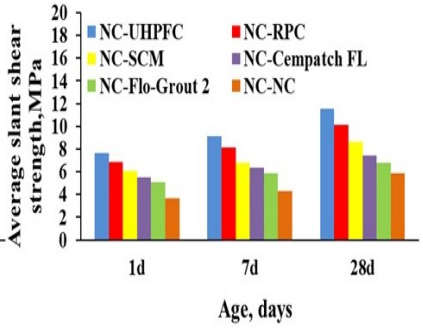

Fig. 8. Average slant shear strengths for the drill holes substrate surface.

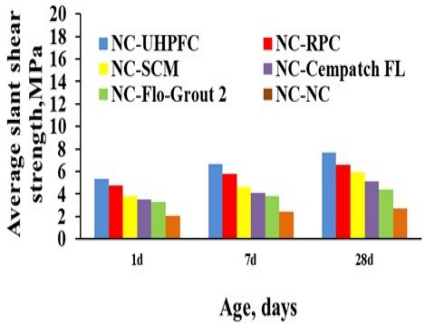

Fig. 9. Average slant shear strengths for the as-cast substrate surface.

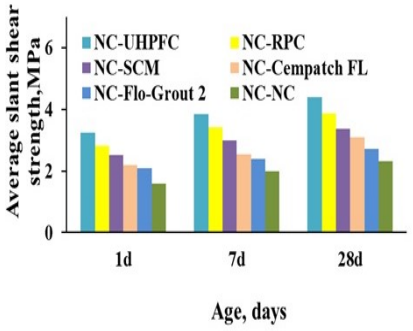

Fig. 10. Average bi-surface shear strengths for the grooved substrate surface.

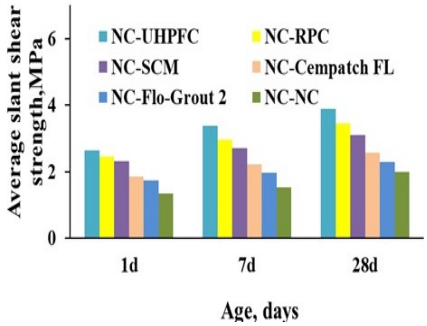

Fig. 11. Average bi-surface shear strengths for the drill holes substrate surface.

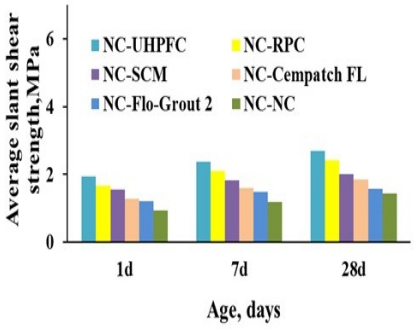

Fig. 12. Average bi-surface shear strengths for the as-cast substrate surface.

Among all the NC substrate-overlay specimens, NC-UHPFC specimens exhibited the highest bond strengths at the three tested ages, while the bond quality decreases with the rest composite specimens in the next order: NC-RPC, NC-SCM, NC- Cempatch FL, NC- Flo-Grout 2 and NC-NC. This indicates that the overlay materials have a significant effect on the bond strength owing to their ability to fill the pores on the surface of substrate, which improve the capillary absorption in the substrate and the adequate contact area between NC substrate and the overlay material. In addition, the grooved and drill holes specimens show a definite increase in the bond strength and out of these two surface preparation specimens, the grooved specimens exhibited the higher bond strength. On the contrary, the specimens with as-cast surface treatment have the lowest bond strength. A possible explanation for this increase in the bond strength of the grooved specimens could be that these specimens provided better interlock between the overlay and NC substrate. Furthermore, as can be seen from the test results, the bond strength increased with the increase of curing age of the composite specimens.

The ratios of the average measured bond strengths by slant shear test to those average measured bond strengths by the bi-surface shear test are shown in Figs. 13, 14, and 15. The slant shear test for grooved-roughness surface resulted in bond strengths that were on average of 2.5, 2.6, and 2.9 times higher than the bond strengths by bi-surface shear test. Whereas, the slant shear test for drill holes, resulted in bond strengths that were on average of 2.3, 2.5, and 2.7 times higher than the bond strengths by bi-surface shear test at ages of 1, 7, and 28 days respectively. For the composite specimens constructed as-cast, a similar trend exists for all tested ages in the case that, the average values of the ratios of the bond strengths of slant shear test to those of bi-surface shear test were 1.8, 1.8, and 1.9 at ages of 1, 7, and 28 days, respectively. Compared to the bi-surface shear, the slant shear result in higher bond strength values, similar results have been obtained by Momayez et al. [23].

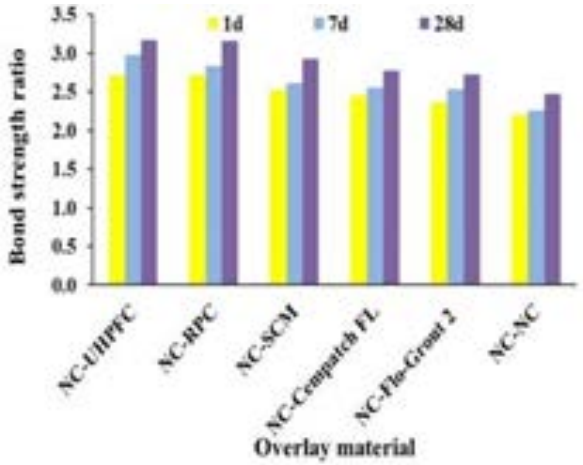

Fig. 13. Ratios of average bond strengths by slant shear test to those of bi-surface test for the grooved substrate surface.

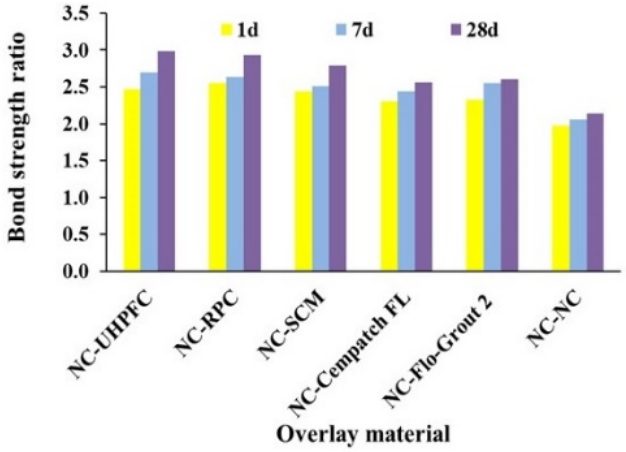

Fig. 14. Ratios of average bond strengths by slant shear test to those of bi-surface test for the drill holes substrate surface.

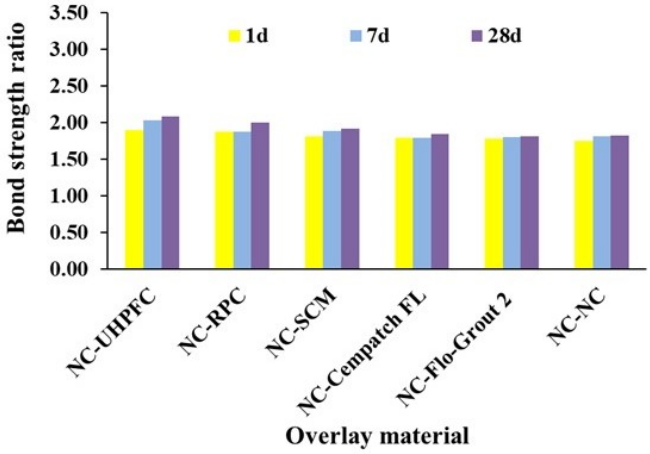

Fig. 15. Ratios of average bond strengths by slant shear test to those of bi-surface test for the as-cast substrate surface.

3.2. The coefficient and angle of friction

The friction of the composite specimens represents the degree of the shearing resistance at the bond interface. The sliding failure is accomplished by the combination of shear and normal stresses as Eq. (2) expresses

$$\tau = c + \mu\sigma_n \tag{2}$$

In which τ is the shear stress at the bond interface (MPa), C is the cohesion (MPa), μ is the friction coefficient, and σ_n is the normal stress at the bond interface (MPa). The normal stress σ_n and the shear stress τ are calculated depends on Eqs. (3) and (4):

$$\tau = \frac{P}{A}cos^2\alpha \tag{3}$$

$$\tau = \frac{P}{A} cos\alpha \; sin\alpha \tag{4}$$

C and σ_n values that obtained through the bi-surface shear test and slant shear test have been used to calculate μ for the composite specimens from Eq. (2), then μ has been used to calculate the friction angle ($\emptyset$) using Eq. (5):

$$\emptyset = \; tan^{-1}\mu \tag{5}$$

The calculated values of μ and $\emptyset$ (in degree) of the studied specimens are summarized in Tables 2, 3, and 4. The results indicate that there was an increase in the μ values between the substrate and the overlay of the grooved surface specimens in comparison with drill holes and as cast specimens. The values of μ varied from 0.91 to 1.21, 0.84 to 1.17 and 0.68 to 0.89 for the grooved, the drill holes and as cast substrate specimens respectively. Similarly, the grooved surface specimens had the highest values of friction angle as compared with the drill holes and as cast substrate specimens. The values of the friction angles varied from 42.30 to 50.42, 40.0 to 49.50 and 34.20 to 41.67 for the grooved, the drill holes and the as-cast substrate specimens, respectively. The results of μ and $\emptyset$ indicate that the increase in the μ and $\emptyset$ values is a result of substrate surface preparation type and interlock effects between the concrete substrate and the overlay.

Table 2. The coefficient of friction μ and the friction angle Ø (degree) for the grooved substrate surface specimens.

Composite specimen	Specimen No.	Age, days					
		1		7		28	
		μ	$\emptyset$	μ	$\emptyset$	μ	$\emptyset$
NC-NC	1	0.94	43.23	0.97	44.13	1.01	45.30
	2	0.91	42.30	0.97	44.13	1.06	46.67
	3	0.93	42.90	0.95	43.53	1.02	45.57
NC-UHPFC	1	1.06	46.67	1.13	48.50	1.17	49.48
	2	1.10	47.72	1.16	49.23	1.21	50.42
	3	1.12	48.24	1.15	49.00	1.18	49.72
NC-RPC	1	1.07	46.94	1.10	47.72	1.15	49.00
	2	1.12	48.24	1.14	48.74	1.18	49.72
	3	1.09	47.47	1.13	48.50	1.18	49.72
NC-SCM	1	1.05	46.40	1.09	47.46	1.13	48.50
	2	1.02	45.57	1.04	46.12	1.14	48.74
	3	1.06	46.67	1.08	47.20	1.16	49.23
NC-Cempatch FL	1	1.00	45.00	1.08	47.20	1.14	48.74
	2	1.04	46.12	1.04	46.12	1.09	47.46
	3	1.02	45.57	1.04	46.12	1.10	47.73
NC- Flo-Grout 2	1	0.97	44.13	1.06	46.67	1.10	47.72
	2	1.00	45.00	1.06	46.67	1.11	48.00
	3	1.03	45.85	1.02	45.57	1.08	47.20

Table 3. The coefficient of friction μ and the friction angle Ø (degree) for the drill holes substrate surface specimens.

Composite specimen	Specimen No.	Age, days					
		1		7		28	
		μ	Ø	μ	Ø	μ	Ø
NC-NC	1	0.86	40.70	0.87	41.00	1.02	45.57
	2	0.84	40.00	0.89	41.67	0.87	41.00
	3	0.86	40.70	0.92	42.60	0.86	40.70
NC-UHPFC	1	1.05	46.40	1.08	47.20	1.15	49.00
	2	1.07	46.94	1.11	48.00	1.17	49.50
	3	1.04	46.12	1.08	47.20	1.15	49.00
NC-RPC	1	1.01	45.29	1.10	47.72	1.15	49.00
	2	1.04	46.12	1.05	46.40	1.16	49.24
	3	1.04	46.12	1.07	46.67	1.12	48.24
NC-SCM	1	1.05	46.40	1.04	46.12	1.12	48.24
	2	1.00	45.00	1.03	45.85	1.08	47.20
	3	1.02	45.57	1.06	46.67	1.14	45.74
NC-Cempatch FL	1	0.95	43.53	1.01	45.29	1.04	46.12
	2	1.02	45.57	1.00	45.00	1.06	46.67
	3	0.96	43.83	1.05	46.40	1.07	46.94
NC- Flo-Grout 2	1	0.93	42.92	1.03	45.85	1.10	47.73
	2	1.02	45.57	1.09	47.47	1.03	45.85
	3	0.98	44.42	1.05	46.40	1.07	46.94

Table 4. The coefficient of friction μ and the friction angle Ø (degree) for the as-cast substrate surface specimens.

Composite specimen	Specimen No.	Age, days					
		1		7		28	
		μ	Ø	μ	Ø	μ	Ø
NC-NC	1	0.71	35.37	0.72	35.75	0.75	36.87
	2	0.71	35.37	0.75	36.87	0.76	37.23
	3	0.68	34.20	0.75	36.87	0.77	37.60
NC-UHPFC	1	0.83	39.70	0.86	40.70	0.89	41.67
	2	0.81	39.00	0.88	41.35	0.89	41.67
	3	0.82	39.35	0.82	39.35	0.88	41.35
NC-RPC	1	0.80	38.66	0.83	39.70	0.83	39.70
	2	0.74	36.50	0.83	39.70	0.84	40.00
	3	0.79	38.31	0.79	38.31	0.89	41.67
NC-SCM	1	0.75	36.87	0.81	39.00	0.80	38.66
	2	0.74	36.50	0.77	37.60	0.82	39.35
	3	0.75	36.87	0.88	41.35	0.82	39.35
NC-Cempatch FL	1	0.73	36.13	0.75	36.87	0.76	37.23
	2	0.75	36.87	0.79	38.31	0.78	37.95
	3	0.76	37.23	0.79	38.31	0.83	39.70
NC- Flo-Grout 2	1	0.76	37.23	0.74	36.50	0.78	37.95
	2	0.74	36.50	o.77	37.60	0.79	38.31
	3	0.73	36.13	0.79	38.31	0.75	36.87

3.3. The failure modes

The quality of the bond between the NC substrate and the overlay material can be expressed by the location of the failure; this failure can be represented by different failure modes that were visually examined and recorded. The failure modes were classified into four types, the interfacial bond failure (FM1), interfacial failure and small parts broken in the substrate (FM2), the substrate fracture (FM3) and complete substratum failure (FM4). Most of the failure modes in the slant shear test and bi-surface shear test occurred throughout the NC substrate and small cracks in the overlay concrete for the grooved and the drill holes substrate surface. Whereas, the majority of the failure modes took place throughout the interface for the as cast composite specimens due to insufficiency friction between the substrate and the overlay. Besides, in some cases, the interface failure occurred after the fracture in the NC substrate or the failure happened in the NC substrate and no separation between the NC substrate and the overlay especially in the NC-UHPFC and NC-RPC specimens, which indicates that the bond strength between NC substrate and the overlay is strong.

4. Conclusions

The outcomes of this study confirmed a number of key conclusions about bond strength performance between the normal concrete substrate and different overlay materials; which could be summarised as follows:

- The different overlay materials have different effectiveness contributing on the bond performance. The measured bond strength between NC substrate and different overlay materials decrease in the following order: NC-UHPFC, NC-RPC, NC-SCM, NC- Cempatch FL, NC- Flo-Grout 2 and NC-NC. Thus, the result of the slant shear strength test and bi-surface shear strength test show that the UHPFC has a very good bond quality with the NC substrate and it is adequate for overlay applications.
- The bond strength is significantly influenced by the used test method. Whilst the bond strengths from the slant shear test were up to two-three times larger than that from the bi-surface shear test. It is essential to choose the bond tests that they enable to simulate the actual state of shear stress that the structures are subjected to.
- The highest bond strengths are achieved for the grooving surfaces in comparison with the drill holes and as-cast treatments at the three tested ages.
- For all tested specimens, the bond strength increased as the curing age of the composite specimens increased.
- The results of the calculated values of friction coefficient μ and friction angle $\emptyset$ (degree) are dependent on the type of surface treatment. The grooved surface treatment indeed leads to higher calculated values of μ and $\emptyset$ than the calculated values of μ and $\emptyset$ of both drill holes and as-cast surface treatments.
- The majority of the failure modes in the slant shear and bi-surface shear tests were through the NC substrate, which indicate that the cracking strength of the NC substrate is lower than the bond strength between NC substrate and overlay materials.

Nomenclatures

A	Bonded surface area, mm^2
C	Cohesion, MPa
F	Maximum applied force, N
f_s	Bond shear strength, MPa

Greek Symbols

μ	Friction coefficient
σ_n	Normal stress at the bond interface, MPa
τ	Shear stress at the bond interface, MPa
$\emptyset$	Friction angle, degree

Abbreviations

CA	Coarse aggregate
Cempatch FL	Shrinkage compensated micro concrete
FA	Fine aggregate
Flo-Grout 2	Non-shrink cementitious
LP	Limestone powder
MSF	Micro steel fibers
NC	Normal strength concrete
PLC	Portland limestone cement
RPC	Self-compacting mortar
SCM	Self-compacting mortar
SF	Silica fume
UHPEC	Ultra- high performance fiber concrete

References

1. Carbonell Muñoz, M.A.; Harris, D.K.; Ahlborn, T.M.; and Froster, D.C. (2014). Bond performance between ultrahigh-performance concrete and normal-strength concrete. *Journal of Materials in Civil Engineering*, 26(8), 401-4031.
2. Aulawi, H.; Farida, I.; Nandiyanto, A.B.D.; Abdullah, C.U.; and Widiaty, I. (2020). Effect of micro-scaled size of sand on concrete solidity and compressive strength. *Journal of Engineering Science and Technology* (*JESTEC*), 15(3), 1815-1823.
3. Majdi, H.S.; Shubbar, A.A.F.; Nasr, M.S.; Al-Khafaji, Z.S.; Jafer, H.; Abdulredha, M.; Al-Masoodi, Z.; Sadique, M.M.; and Hashim, K.S. (2020). Experimental data on compressive strength and ultrasonic pulse velocity properties of sustainable mortar made with high content of GGBFS and CKD combinations. *Data in Brief*, 31, 105961-105972.
4. Saldanha, R.; Júlio, E.; Dias-da-Costa, D.; and Santos, P. (2013). A modified slant shear test designed to enforce adhesive failure. *Construction and Building Materials*, 41, 673-680.
5. Shubbar, A.A.; Al-Shaer, A.; AlKizwini, R.S.; Hashim, K.; Hawesah, H.A.; and Sadique, M. (2019). Investigating the influence of cement replacement by high volume of GGBS and PFA on the mechanical performance of cement

mortar. *International Conference on Civil and Environmental Engineering Technologies (ICCEET)*, University of Kufa, Iraq, 31-38.

6. Shubbar, A.A.; Jafer, H.; Dulaimi, A.; Hashim, K.; Atherton, W.; and Sadique, M. (2018). The development of a low carbon binder produced from the ternary blending of cement, ground granulated blast furnace slag and high calcium fly ash: An experimental and statistical approach. *Construction and Building Materials*, 187, 1051-1060.
7. Santos, P.D.S.; and Júlio, E.N.B.S. (2011). Factors affecting bond between new and old concrete. *ACI Materials Journal*, 108(4), 449-458.
8. Shen, Y.; Wang, Y.; Yang, Y.; Sun, Q.; Luo, T.; and Zhang, H. (2019). Influence of surface roughness and hydrophilicity on bonding strength of concrete-rock interface. *Construction and Building Materials*, 213, 156-166.
9. Valikhani, A.; Jahromi, A.J.; Mantawy, I.M.; and Azizinamini, A. (2020). Experimental evaluation of concrete-to-UHPC bond strength with correlation to surface roughness for repair application. *Construction and Building Materials*, 238 (2), 753-768
10. Chilwesa, M.; Minelli, F.; Reggia, A.; and Plizzari, G. (2017). Evaluating the shear bond strength between old and new concrete through a new test method. *Magazine of Concrete Research*, 60(1), 377-390.
11. Kadhim, A.; Sadique, M.; Al-Mufti, R.; and Hashim, K. (2020). Long-term performance of novel high-calcium one-part alkali-activated cement developed from thermally activated lime kiln dust. *Journal of Building Engineering*, 32, 1-17.
12. Kadhim, A.; Sadique, M.; Al-Mufti, R.; and Hashim, K. (2020). Developing one-part alkali-activated metakaolin/natural pozzolan binders using lime waste as activation agent. *Advances in Cement Research*, 32(11), 1-38.
13. Shubbar, A.A.; Sadique, M.; Nasr, M.S.; Al-Khafaji, Z.S.; and Hashim, K.S. (2020). The impact of grinding time on properties of cement mortar incorporated high volume waste paper sludge ash. *Karbala International Journal of Modern Science*, 6(3), 1-23.
14. Tayeh, B.A.; Abu-Bakar, B.H.; and Johari, M.A.M. (2013). Characterization of the interfacial bond between old concrete substrate and ultra high performance fiber concrete repair composite. *Materials and structures*, 46(5), 743-753.
15. Shubbar, A.A.; Sadique, M.; Shanbara, H.K.; and Hashim, K. (2020). *The* development of a new low carbon binder for construction as an alternative to cement. *Advances in Sustainable Construction Materials and Geotechnical Engineering* (1st ed.). Berlin: Springer.
16. He, S.; Mosallam, A.S.; Fang, Z.; Sun, X.; and Su, J. (2018). Experimental evaluation of shear connectors using reactive powder concrete under natural curing condition. *Construction and Building Materials*, 191(3), 775-786.
17. Farzad, M.; Shafieifar, M.; and Azizinamini, A. (2019). Experimental and numerical study on bond strength between conventional concrete and Ultra High-Performance Concrete (UHPC). *Engineering Structures*, 186, 297-305.
18. Eyre, J.; and Campos, E.S. (1996). Upper bounds in the slant shear testing of perfectly plastic joints in concrete. *Magazine of Concrete Research*, 48(176), 181-188.

19. Omer, G.; Kot, P.; Atherton, W.; Muradov, M.; Gkantou, M.; Shaw, A.; Riley, M.L.; Hashim, K.S.; and Al-Shamma'a, A. (2020). A non-destructive electromagnetic sensing technique to determine chloride level in maritime concrete. *Karbala International Journal of Modern Science,* 6(4), 1-14.
20. Mirmoghtadaei, R.; Mohammadi, M.; Samani, N.A.; and Mousavi, S. (2015). The impact of surface preparation on the bond strength of repaired concrete by metakaolin containing concrete. *Construction and Building Materials,* 80(1), 76-83.
21. Diab, A.M.; Elmoaty, A.M.; and Tag, M.R. (2017). Slant shear bond strength between self compacting concrete and old concrete. *Construction and Building Materials*, 130(2), 73-82.
22. Momayez, A.; Ramezanianpour, A.A.; Rajaie, H.; and Ehsani, M.R. (2004). Bi-surface shear test for evaluating bond between existing and new concrete. *Materials Journal,* 101(2), 99-106.
23. Momayez, A.; Ehsani, M.R.; Ramezanianpour, A.A.; and Rajaie, H. (2005). Comparison of methods for evaluating bond strength between concrete substrate and repair materials. *Cement and Concrete Research,* 35(4), 748-757.
24. De La Varga, I.; Munoz, J.F.; Bentz, D.P.; Spragg, R.; Stutzman, P.; and Graybeal, B. (2018). Grout-concrete interface bond performance: Effect of interface moisture on the tensile bond strength and grout microstructure. *Construction and Building Materials,* 170, 747-756.
25. Mirmoghtadaei, R.; Mohammadi, M.; Samani, N.A.; and Mousavi, S. (2015). The impact of surface preparation on the bond strength of repaired concrete by metakaolin containing concrete. *Construction and Building Materials,* 80(2), 76-83.
26. Costa, H.; Carmo, R.F.; and Júlio, E. (2018). Influence of lightweight aggregates concrete on the bond strength of concrete-to-concrete interfaces. *Construction and Building Materials*, 180(2), 519-530.
27. Standard, S.I. (2003). *ASTM C33 standard specification for concrete aggregates*, National laboratories, Pennsylvania.
28. Standards, S.I. (2013). *ASTM C494 standard specification for chemical admixtures for concrete*, National laboratories, Pennsylvania.
29. Standards, S.I. (2012). *ASTM C09 standard specification for portland cement*, National laboratories, Pennsylvania.
30. Tuaum, A.; Shitote, S.; and Oyawa, W. (2018). Experimental study of self-compacting mortar incorporating recycled glass aggregate. *Buildings*, 8(2), 15-23.
31. Standard, S.I. (2005). *ASTM C882/C882M standard test method for bond strength of epoxy-resin systems used with concrete by slant shear*, National laboratories, Pennsylvania.
32. Beushausen, H.; Höhlig, B.; and Talotti, M. (2017). The influence of substrate moisture preparation on bond strength of concrete overlays and the microstructure of the OTZ. *Cement and Concrete Research*, 92, 84-91.